J. Biochem. 131, 785–790 (2002)

Irreversible Photobleaching of Bacteriorhodopsin in a High-Temperature Intermediate State[1]

Yasunori Yokoyama,[2] Masashi Sonoyama, and Shigeki Mitaku

Department of Biotechnology, Tokyo University of Agriculture and Technology, 2-24-16 Nakacho, Koganei, Tokyo 184-8588

Received February 14, 2002; accepted March 20, 2002

The photo-intermediate state of bacteriorhodopsin is a metastable state that spontaneously transforms to the ground state over the energy barrier of a local minimum. As the recovery of the photocycle to the ground state and irreversible photobleaching to the denatured state may occur from the same local energy minimum, depending on the temperature, the structural stability of bacteriorhodopsin under illumination at high temperature was measured in order to study the intra- and inter-molecular interactions that contribute to the recovery of the ground state. Visible CD spectra of bacteriorhodopsin began to change at 60°C from a bilobed to positive type in accordance with an appearance of an absorption peak at 470 nm. Irreversible photobleaching, the light-induced denaturation, also started to occur at 60°C, suggesting some correlation between irreversible photobleaching and the structural change to the high-temperature intermediate state. However, bacteriorhodopsin in the dark was stable up to 70°C, suggesting that there is some additional factor that lends structural stability to bacteriorhodopsin in the dark. The contribution of protein–protein interactions to stability is discussed on the basis of the difference in the denaturation behaviors between light and dark conditions.

Key words: bacteriorhodopsin, high-temperature intermediate state, irreversible photobleaching, protein–protein interaction, thermal denaturation.

Bacteriorhodopsin (bR), found in the cytoplasmic membrane of *Halobacterium salinarum*, is a light-driven proton pump (*1*). bR molecules spontaneously form a two-dimensional (2D) crystal called purple membrane in the plasma membrane (*2*). Many studies of the proton pumping mechanism of bR have been reported, revealing the function of bR to comprise several photo-intermediate states (J, K, L, M, N, and O) (*3, 4*). The charge distributions and hydrogen bonding networks, which include several water molecules in the transmembrane region, are altered in the photo-intermediate states, as revealed by vibrational spectroscopic studies (*5–8*). Furthermore, the three-dimensional (3D) structures of the photo-intermediates of bR have recently been reported (*9–15*), leading to a hypothesis of structural switching during the photocycle. The Schiff base is closed on the cytoplasmic side in the ground state (*16–22*), while the structure switches to the open state during the M and N intermediate states (*9, 11, 13, 14*), resulting in vectorial proton pumping. However, the mechanism of the structural stability of the closed and open states, as well as the switching mechanism, remains to be revealed.

The stabilization factors of the 3D structure of bR in the ground state have been extensively investigated through denaturation experiments in the dark. The results indicate that polar interactions, particularly hydrogen bonding interactions and ion pairing, are essential for the stability of the ground state of bR (*23, 24*). Two kinds of intermediate states have been investigated to date, a high-temperature intermediate state and the photo-intermediate states. The structure of bR is highly stable with respect to heat in the dark, however, two thermal transitions at 80 and 95°C have been identified by differential scanning calorimetry (*25–27*). The lower transition corresponds to the melting of the 2D crystalline structure (*25, 28*), while the real denaturation of bR in the dark occurs at the higher transition, just below the boiling temperature of water (*25–27*). Furthermore, prior to 2D crystal melting in the dark, bR molecules undergo structural changes that can be monitored *via* blue-shift in the absorption spectrum, red-shift in the intrinsic fluorescence, and changes in the infrared spectrum (*25–27, 29*). These spectral changes correspond to an increase in *cis*-form retinal, conformational changes of this protein around tryptophan residues, and α_{II}-to-α_{I} transition of the transmembrane helices, respectively (*25–27, 29*).

Denaturation experiments on bR under illumination have also been carried out (*30–32*). Etoh *et al.* (*30*) showed that irreversible photobleaching, light-induced denaturation, occurs just above the melting temperature of the 2D crystal. Mukai *et al.* (*31*) reported that bR solubilized by octyl-β-glucoside also undergoes irreversible photobleaching, even at room temperature. Dancsházy *et al.* (*32*) examined the photobleaching of bR under various pH, temperature, light intensity and light exposure conditions for the purpose of developing practical devices. The experimen-

[1]This work was supported in part by a Grant-in-Aid from the Ministry of Education, Culture, Sports, Science and Technology (Monbukagakusho).

[2]To whom correspondence should be addressed. Phone/Fax: +81-42-388-7464, E-mail: yokoyama@proteome.bio.tuat.ac.jp

Abbreviation: bR, bacteriorhodopsin.

tal results suggested that the structural stability of the photo-intermediates is lower than that of the ground state. However, the specific physical factors that determine the photo- and high-temperature intermediate states have yet to be identified.

In the present work, we investigated the denaturation of bR by absorption and circular dichroism (CD) spectroscopy under various temperature and light illumination conditions. We found that irreversible photobleaching of bR begins at 60°C at which temperature native bR begins to transform into a stable high-temperature intermediate state in the dark. However, thermal denaturation in the dark did not occur below 70°C despite the appearance of the high-temperature intermediate. Analysis of the denaturation kinetics showed that light illumination significantly enhanced the structural decay of bR and generated a fast decay component. We discuss the contribution of intramolecular and protein–protein interactions to the stabilization of the intermediate states.

MATERIALS AND METHODS

Purple membranes of *Halobacterium salinarum*, strain R1M1, were isolated and purified according to the standard procedure (*33*). The purified purple membranes were suspended in 50 mM Tris-HCl buffers (pH 7.0), with the pH titrated at each temperature with an HCl solution. The concentration of bR used for spectral measurements was approximately 5 μM. The protein concentration was determined from the absorption maximum at 568 nm using an extinction coefficient of 62,700 ± 700 $M^{-1}\cdot cm^{-1}$ (*34*).

Absorption spectra at high temperature in the dark were recorded using a photo-diode array spectrophotometer with a thermostated cell holder (DU7500, Beckman Coulter, USA). Visible CD spectra were measured using a spectropolarimeter (J-820, Jasco, Tokyo) with a thermostated cell holder in the temperature range 25 to 90°C.

Absorption spectra under visible light were recorded using a light illumination system, consisting of a Xe lamp source (average light power: 200 $mW\cdot cm^{-2}$), a color filter (Y52) to filter out light shorter than 520 nm, a heat-cut filter to prevent heating by irradiation, convex lenses, and a mirror (*30*).

Visible CD spectra were recorded 5 min after the temperature jump. In order to investigate the reversibility of the spectral changes, the samples were incubated for 1 h, and

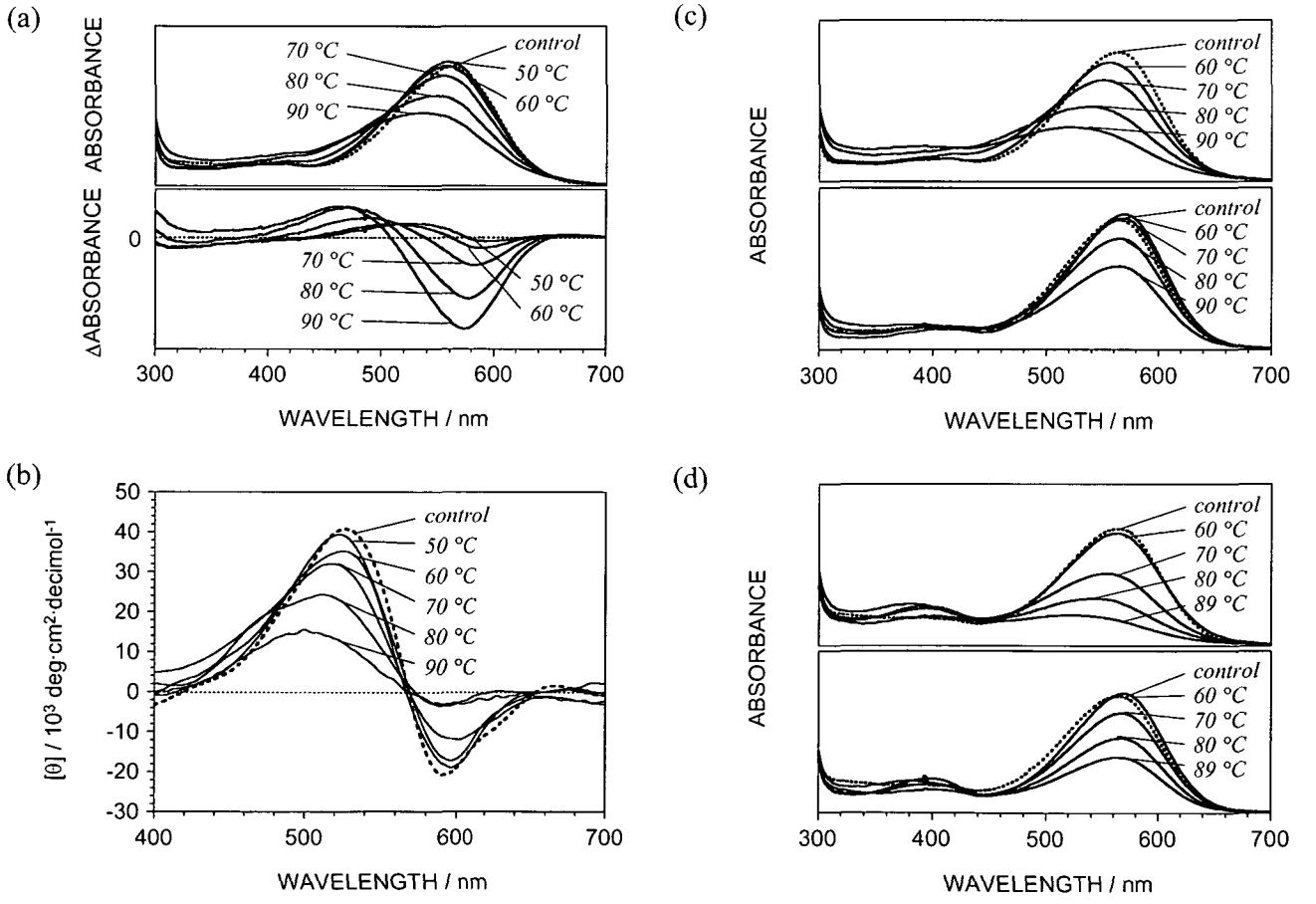

Fig. 1. **(a) Absorption spectra of bacteriorhodopsin after incubation for 5 min at high temperatures in the dark (upper), and the difference spectra for bacteriorhodopsin from the standard spectrum at 25°C (lower). (b) Visible CD spectra of bacteriorhodopsin, after incubation for 5 min in the dark. (c) Absorption spectra of bacteriorhodopsin after incubation for 1 h in the dark (upper), and absorption spectra immediately after cooling (lower). (d) Absorption spectra of bacteriorhodopsin after illuminated incubation for 1 h (upper), and absorption spectra immediately after cooling (lower).** Control curves indicate spectra measured at 25°C before the temperature jump.

then cooled in ice water immediately following measurements at high temperature. Absorption spectra measurements were then performed at room temperature. The degree of reversibility of the absorption spectral change that occurred during high-temperature incubation was calculated by dividing the absorbance at around 560 nm after cooling by the absorbance prior to heating. Temperature conditions under illumination were the same as those in the dark. Baseline correction of absorption spectra was performed to eliminate the scattering effect from the spectra by subtracting the power function of the wavelength.

In absorption kinetics measurements, absorption spectra were measured successively at intervals of 150 s both in the dark and under illumination. Kinetics analyses were performed using a KaleidaGraph (Synergy Software, USA). All data could be fitted to single- or double-exponential decay curves with correlation coefficients as large as 0.999.

RESULTS

Absorption spectra, obtained in the dark 5 min after temperature jump are shown in Fig. 1a. The final temperatures were in the range 50 to 90°C. The absorption spectra ex-

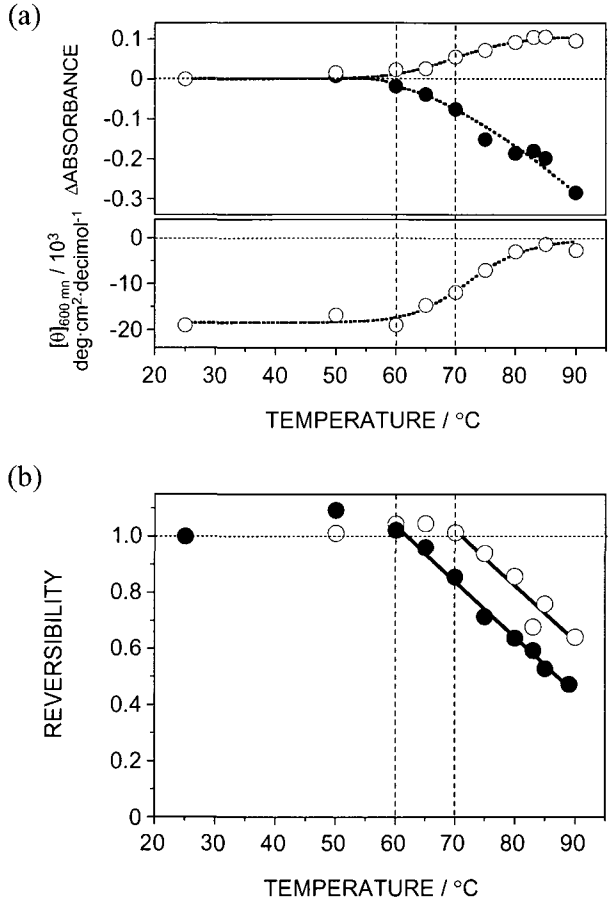

Fig. 2. **(a) Temperature dependence of the difference absorption at 470 nm (open circles) and 570 nm (closed circles), and temperature dependence of the visible CD at 600 nm (lower). (b) Temperature dependence of the reversibility of absorption spectral intensities after cooling in the dark (open circles) and under illumination (closed circles).**

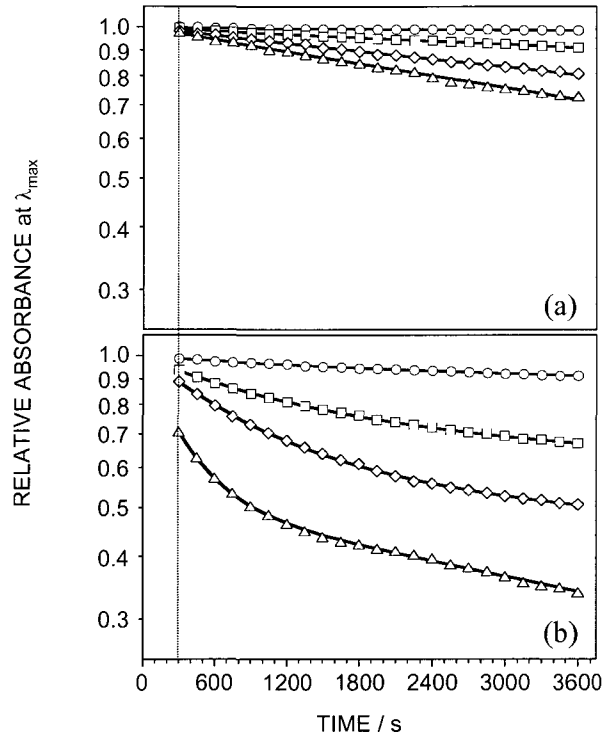

Fig. 3. **(a) Decay curves of the relative absorbance at maximum wavelengths around 560 nm in the dark at various temperatures: 60°C (circles), 70°C (squares), 80°C (diamonds), and 85°C (triangles). (b) Decay curves of the relative absorbance at maximum wavelengths around 560 nm under illumination at various temperatures: 60°C (circles), 70°C (squares), 80°C (diamonds), and 85°C (triangles).**

TABLE I. **Kinetic parameters of photobleaching and thermal denaturation of bacteriorhodopsin in the dark.**

Temperature (°C)	τ_D[a] (s^{-1})	τ_{L1}[b] (s^{-1})	Proportion of τ_{L1} (%)	τ_{L2}[b] (s^{-1})	Proportion of τ_{L2} (%)
60		1.12×10^{-3}	2.33	1.93×10^{-5}	97.7
65		4.77×10^{-4}	6.03	2.24×10^{-5}	94.0
70	2.59×10^{-5}	7.50×10^{-4}	21.8	3.32×10^{-5}	78.2
75	2.60×10^{-5}	9.98×10^{-4}	31.2	3.36×10^{-5}	68.8
80	6.05×10^{-5}	1.22×10^{-3}	44.8	6.64×10^{-5}	55.2
83	7.06×10^{-5}	2.38×10^{-3}	48.7	7.96×10^{-5}	51.3
85	9.21×10^{-5}	2.79×10^{-3}	48.5	1.15×10^{-4}	51.5
89		2.74×10^{-3}	47.2	2.48×10^{-4}	52.8
90	8.90×10^{-5}				

[a]τ_D, decay constant of the thermal denaturation kinetics in the dark. [b]τ_{L1} and τ_{L2}, decay constants of the fast and slow components of photobleaching.

hibit a gradual blue-shift from 560 nm at 50°C to 540 nm at 90°C. The maximum absorbance decreased at high temperatures in accordance with the change in the maximum wavelength. The difference spectra in Fig. 1a indicate that the absorption at 570 nm decreases with increasing temperature, concomitant with an increase in the absorption at 470 nm. Figure 1b shows visible CD spectra 5 min after temperature jump to various final temperatures. The negative peak in the bilobed spectrum at room temperature gradually smears out with increasing temperature. The CD spectra above 80°C exhibits a positive type CD band centered at 500 nm. Both absorption and visible CD spectra in the dark reveal structural changes above 60°C. In order to separate the reversible and irreversible components of the spectral changes, we also measured the absorption spectra in the dark (Fig. 1c) and under illumination (Fig. 1d) after quenching the high-temperature samples. The spectra at 60°C recovered completely at room temperature, indicating that there is no irreversible component of the spectral change below 60°C. However, there is a significant difference in the recovery of the spectra above 60°C under illumination. The spectral change was completely reversible even at 70°C in the dark, whereas there was a large irreversible component at 70°C under illumination. This suggests that the protein has an intermediate state between the native and denatured states in this temperature range. A comparison of Fig. 1, c and d, reveals that the denaturation was triggered by light absorption above 60°C, indicating that irreversible photobleaching of bR occurs above this temperature.

The onset of the structural change around 60°C is clear in Fig. 2a. Figure 2b shows the temperature dependence of the reversibility of the absorption spectra in the dark as well as under illumination. The irreversible component of the spectral change as estimated by the quenching experi-

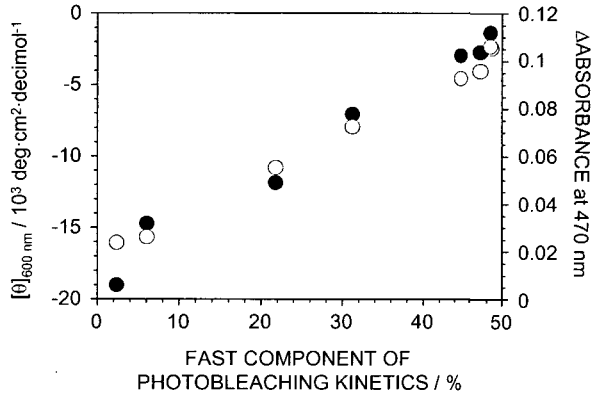

Fig. 4. **Correlation between the proportion of the fast decay component of the photobleaching kinetics and the structural changes in bacteriorhodopsin observed above 60°C in the dark.** Two parameters characterizing the structural changes are plotted: molar ellipticity at 600 nm (closed circles) and difference absorbance at 470 nm (open circles).

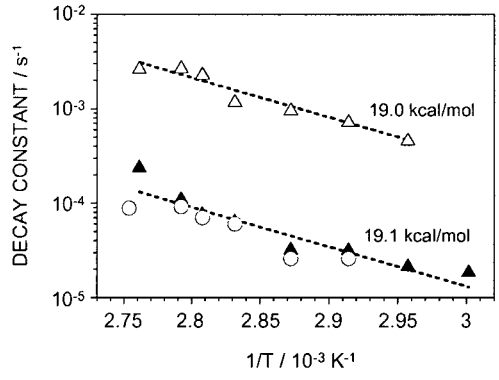

Fig. 5. **Arrhenius plot of the denaturation of bacteriorhodopsin in the dark (circles), and the fast (open triangles), and slow components (closed triangles) under illumination.**

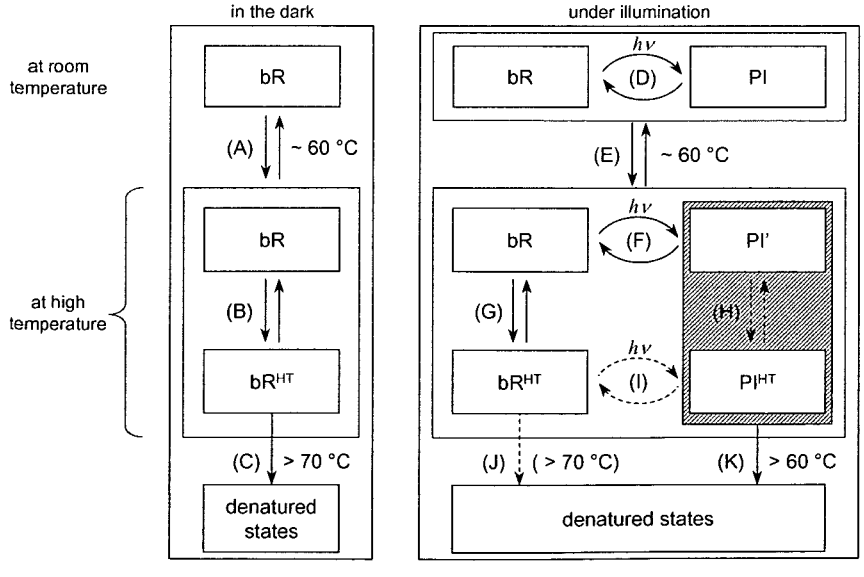

Fig. 6. **Schematic diagram of the structural changes in bR induced by light absorption and heat.** (A) Structural changes in the ground state (bR) in the dark with temperature elevation. (B) Coexistence of the ground state at high temperature and the high-temperature intermediate state (bR^{HT}) in the dark. (C) Denaturation in the dark. (D) Light-induced structural changes in the photo-intermediate states (PI) under physiological conditions (photocycle). (E) Structural changes under illumination with temperature elevation. (F) Light-induced structural changes to the photo-intermediate states at high temperature (PI'). (G) Coexistence of the ground state at high temperature and the high-temperature intermediate state under illumination. (H) Coexistence of photo-intermediate states at high temperature and photo-intermediates from the high-temperature intermediate (PI^{HT}). (I) Light-induced structural changes to photo-intermediate states from the high-temperature intermediate state. (J) Denaturation from the high-temperature intermediate state under illumination. (K) Irreversible photobleaching from photo-intermediates at high temperature. The solid arrows indicate reasonable reactions; the broken arrows indicate plausible reactions for which sufficient evidence is unavailable.

ments occurs at 60°C under illumination, which is about 10°C lower than the corresponding temperature in the dark. Irreversible photobleaching and structural changes in the dark were then recorded at the same temperature (Fig. 2a).

We measured the decay kinetics of the absorbance at the spectral peak around 560 nm in order to elucidate the difference between photobleaching and denaturation in the dark. The time courses of the relative absorbance in the dark and under illumination are shown in Fig. 3, a and b, respectively. Only the data points after the dead time of 300 s are shown. It was possible to reproduce the decay of the relative absorbance in the dark using a single-exponential decay curve. The decay time in the dark was found to be on the order of 10^4 s. Under illumination, the temperature jump measurements followed a double-exponential curve and revealed that the slower decay time of photobleaching is very similar to that of the denaturation of bR in the dark. The faster component was observed to be 10 times faster than the slower component. The kinetics parameters obtained by curve fitting are shown in Table I. As shown in Fig. 4, the correlation between the fast component of photobleaching and the structural changes observed in the dark strongly suggests the existence of a correlation between the irreversible photobleaching phenomenon and the structural change to the high-temperature intermediate state.

Figure 5 shows the Arrhenius plot of the denaturation kinetics under illuminated and dark conditions. The decay constants of denaturation in the dark are almost the same as those of the slower decay components under illumination. The two parallel lines in Fig. 5 correspond to activation energies of 19.0 kcal·mol^{-1} for the fast component and 19.1 kcal·mol^{-1} for the slow component. The difference between the illuminated and dark conditions is almost negligible compared the activation energies themselves, although the difference in the frequency factor is large.

DISCUSSION

The experimental results obtained in this study can be summarized as three main points. (i) The structural changes in bR begin at 60°C, as seen in the absorption and visible CD spectra. The absorption spectrum indicates that the state of a single molecule of bR changes above 60°C (*29*), whereas the CD spectrum shows that protein–protein interactions in the 2D crystal begin to decrease at this temperature. (ii) The structure of bR in the dark is stable up to 70°C, whereas irreversible photobleaching begins at 60°C, the temperature at which the structural changes in bR in the dark also begin. This suggests that the stability of bR under illumination is determined by the state of individual molecules and that there is an additional factor that stabilizes the structure of bR in the dark. (iii) Denaturation kinetics revealed that the structure of bR denatures according to a single-exponential decay, and that irreversible photobleaching has two decay components. The decay constant of the slow component of photobleaching is almost the same as that for denaturation in the dark. An Arrhenius plot of the kinetic constants of the fast and slow components gives very similar activation energies of about 19 kcal·mol^{-1}.

On the basis of these experimental results, combined with knowledge from previous reports, plausible reaction processes for bR have been derived, as shown in Fig. 6. Among the three processes shown, (A), (B), and (C), there are numerous papers dealing with changes at around 60°C (process A), as are there on the coexistence of two states, the ground state and the high-temperature intermediate state of bR (process B). The blue-shift in the absorption spectrum above 60°C suggests a conformational change in the retinal chromophore to the *cis* form (*25, 29*). It has also been reported that this spectral change is associated with conformational changes in the transmembrane helices, specifically the α_{II}-to-α_{I} transition (*29*). A fluorescence study of bR at high temperature revealed that the intrinsic fluorescence spectra undergo a red-shift at temperatures above 60°C (*27*). However, this spectral change is relatively small (~5 nm), indicating subtle structural changes around the tryptophan residues (*27*). All the spectral changes above 60°C observed in this work and in previous reports are gradual (*25–29*), indicating that the ground state and the high-temperature intermediate state coexist in the temperature range above 60°C. It has also been reported that the *cis* component of retinal gradually increases above 60°C, confirming the coexistence of the two states. However, we revealed that the onset of denaturation in the dark occurs at 70°C through detailed analysis of the denaturation kinetics. The discrepancy between the onset of structural change and that of denaturation strongly suggests that denaturation in the dark is influenced not only by structural changes in individual bR molecules, but also by protein–protein interactions with neighboring molecules. This discrepancy is reasonable if the high-temperature intermediate states are stabilized by interactions with ground-state bR molecules.

When bR is illuminated by visible light, three different photocycles can occur (processes D, F, and I in Fig. 6), corresponding to the three species of bR existing in the dark (bR below and above 60°C, and the high-temperature intermediate state bR^{HT}). The photocycle below 60°C has been well-studied and is known not to branch to the denaturation process. It has been reported by Wang and El-Sayed (*29*) that the M-intermediate state of the photocycle is observable in the high-temperature range. Therefore, at least one of these photocycles, here F or I, proceeds under illumination. The most plausible process is F, although H and I cannot be discounted. The results of the present work indicate that irreversible photobleaching from the photo-intermediate state PI′ or PI^{HT} occurs above 60°C. In this case, the onset temperature of denaturation coincides with the structural change in bR molecules, suggesting that the irreversible photobleaching phenomenon depends on properties of individual bR molecules. However, considering that protein–protein interactions among neighboring molecules also begins to decrease at 60°C, as judged from the changes in the visible CD spectra obtained in this study, these interactions might contribute to some extent to the stabilization of photo-intermediate states at high temperature.

The decay behavior of the bR structure is related to the reaction scheme under illumination as shown in Fig. 6. Decay in the dark has a single component, which is considered to be the high-temperature intermediate state, whereas the corresponding decay under illumination has two components, one fast and the other slow. The decay constant of the slow component is almost the same as that of the single decay in the dark, providing important infor-

mation for elucidating the reaction scheme of the decay of the two components under illumination. However, it is difficult to form a fundamental reaction equation because photocycle I, the photo-intermediates from the high-temperature intermediate state (PI^{HT}), and reaction H are obscure at present. Measurements of photocycles in the high-temperature range will be necessary to identify photo-intermediate states and elucidate the mechanism of their stability. It should also be noted that knowledge of the conditions under which bR is stable in the dark but unstable under illumination will be useful for studying the forces that restore the photo-intermediate states to the ground state.

REFERENCES

1. Bogomolni, R.A., Baker, R.A., Lozier, R.H., and Stoeckenius, W. (1976) Light-driven proton translocation in *Halobacterium halobium*. *Biochim. Biophys. Acta* **440**, 68–88
2. Henderson, R. and Unwin, P.N.T. (1975) Three-dimensional model of purple membrane obtained by electron microscopy. *Nature* **257**, 28–32
3. Lozier, R.H., Bogomolni, R.A., and Stoeckenius, W. (1975) Bacteriorhodopsin: a light-driven proton pump in *Halobacterium halobium*. *Biophys. J.* **15**, 955–962
4. Lanyi, J.K. (1993) Proton translocation mechanism and energetics in the light-driven pump bacteriorhodopsin. *Biochim. Biophys. Acta* **1183**, 241–261
5. Maeda, A., Sasaki, J., Shichida, Y., Yoshizawa, T., Chang, M., Ni, B., Needleman, R., and Lanyi, J.K. (1992) Structures of aspartic acid-96 in the L and N intermediates of bacteriorhodopsin: analysis by Fourier transform infrared spectroscopy. *Biochemistry* **31**, 4684–4690
6. Sasaki, J., Lanyi, J.K., Needleman, R., Yoshizawa, T., and Maeda, A. (1994) Complete identification of C–O stretching vibrational bands of protonated aspartic acid residues in the difference infrared spectra of M and N intermediates versus bacteriorhodopsin. *Biochemistry* **33**, 3178–3184
7. Rödig, C., Chizhov, I., Weidlich, O., and Siebert, F. (1999) Time-resolved step-scan Fourier transform infrared spectroscopy reveals differences between early and late M intermediates of bacteriorhodopsin. *Biophys. J.* **76**, 2687–2701
8. Kandori, H. (2000) Role of internal water molecules in bacteriorhodopsin. *Biochim. Biophys. Acta* **1460**, 177–191
9. Edman, K., Nollert, P., Royant, A., Belrhali, H., Pebay-Peyroula, E., Hajdu, J., Neutze, R., and Landau, E.M. (1999) High-resolution X-ray structure of an early intermediate in the bacteriorhodopsin photocycle. *Nature* **401**, 822–826
10. Luecke, H., Schorbert, B., Richter, H.-T., Cartailler, J.-P., and Lanyi, J.K. (1999) Structural changes in bacteriorhodopsin during ion transport at 2 angstrom resolution. *Science* **286**, 255–260
11. Sass, H.J., Büldt, G., Gessenich, R., Hehn, D., Neff, D., Schlesinger, R., Berendzen, J., and Ormos, P. (2000) Structural alternations for proton translocation in the M state of wild-type bacteriorhodopsin. *Nature* **406**, 649–653
12. Royant, A., Edman, K., Ursby, T., Pebay-Peyroula, E., Landau, E.M., and Neutze, R. (2000) Helix deformation is coupled to vectorial proton transport in the photocycle of bacteriorhodopsin. *Nature* **406**, 645–648
13. Vonck, J. (2000) Structure of the bacteriorhodopsin mutant F219L N intermediate revealed by electron crystallography. *EMBO J.* **19**, 2152–2160
14. Subramaniam, S. and Henderson, R. (2000) Molecular mechanism of vectorial proton translocation by bacteriorhodopsin. *Nature* **406**, 653–657
15. Luecke, H., Schobert, B., Cartailler, J.-P., Richter, H.-T., Rosengarth, A., Needleman, R., and Lanyi, J.K. (2000) Coupling photoisomerization of retinal to directional transport in bacteriorhodopsin. *J. Mol. Biol.* **300**, 1237–1255
16. Henderson, R., Baldwin, J.M., Ceska, T.A., Zemlin, F., Beckman, E., and Downing, K.H. (1990) Model for the structure of bacteriorhodopsin based on high-resolution electron cryo-microscopy. *J. Mol. Biol.* **213**, 899–929
17. Grigoerieff, N., Ceska, T.A., Downing, K.H., Baldwin, J.M., and Henderson, R. (1996) Electron-crystallographic refinement of the structure of bacteriorhodopsin. *J. Mol. Biol.* **259**, 393–421
18. Essen, L.-O., Siegert, R., Lehmann, W.D., and Oesterhelt, D. (1998) Lipid patches in membrane protein oligomers: Crystal structure of the bacteriorhodopsin-lipid complex. *Proc. Natl. Acad. Sci. USA* **95**, 11673–11678
19. Belrhali, H., Nollert, P., Royant, A., Manzel, C., Rosenbusch, J.P., Landau, E.M., and Pebay-Peyroula, E. (1999) Protein, lipid and water organization in bacteriorhodopsin: A molecular view of the purple membrane at 1.9 Å resolution. *Struct. Fold. Des.* **7**, 909–917
20. Mitsuoka, K., Hirai, T., Murata, K., Miyazawa, A., Kidera, A., Kimura, Y., and Fujiyoshi, Y. (1999) The structure of bacteriorhodopsin at 3.0 Å resolution based on electron crystallography: implication of the charge distribution. *J. Mol. Biol.* **286**, 861–882
21. Luecke, H., Schobert, B., Richter, H.-T., Cartailler, J.-P., and Lanyi, J.K. (1999) Structure of bacteriorhodopsin at 1.55 Å resolution. *J. Mol. Biol.* **291**, 899–911
22. Sato, H., Takeda, K., Tani, K., Hino, T., Okada, T., Nakasako, M., Kamiya, N., and Kouyama, T. (1999) Specific lipid-protein interactions in a novel honeycomb lattice structure of bacteriorhodopsin. *Acta Crystallogr. D. Biol. Crystallogr.* **55**, 1251–1256
23. Mitaku, S., Ikuta, K., Itoh, H., Kataoka, R., Naka, M., Yamada, M., and Suwa, M. (1988) Denaturation of bacteriorhodopsin by organic solvents. *Biophys. Chem.* **30**, 69–79
24. Mitaku, S., Suzuki, K., Odashima, S., Ikuta, K., Suwa, M., Kukita, F., Ishikawa, M., and Itoh, H. (1995) Interaction stabilizing tertiary structure of bacteriorhodopsin studied by denaturation experiments. *Proteins* **22**, 350–362
25. Jackson, M.B. and Sturtevant, J.M. (1978) Phase transitions of the purple membrane of *Halobacterium halobium*. *Biochemistry* **17**, 911–915
26. Brouillette, C.G., Muccio, D.D., and Finney, T.K. (1987) pH dependence of bacteriorhodopsin thermal unfolding. *Biochemistry* **26**, 7431–7438
27. Shnyrov, V.L. and Mateo, P.L. (1993) Thermal transitions in the purple membrane from *Halobacterium halobium*. *FEBS Lett.* **324**, 237–240
28. Hiraki, K., Hamanaka, T., Mitsui, T., and Kito, Y. (1981) Phase transitions of the purple membrane and the brown holo-membrane x-ray diffraction, circular dichroism spectrum and absorption spectrum studies. *Biochim. Biophys. Acta* **647**, 18–28
29. Wang, J.-P. and El-Sayed, M.A. (2000) The effect of protein conformational change from α_{II} to α_{I} on the bacteriorhodopsin photocycle. *Biophys. J.* **78**, 2031–2036
30. Etoh, A., Itoh, H., and Mitaku, S. (1997) Light-induced denaturation of bacteriorhodopsin just above melting point of two-dimensional crystal. *J. Phys. Soc. Jpn.* **66**, 975–978
31. Mukai, Y., Kamo, N., and Mitaku, S. (1999) Light-induced denaturation of bacteriorhodopsin solubilized by octyl-β-glucoside. *Protein Eng.* **12**, 755–759
32. Dancsházy, Z., Tokaji, Z., and Dér, A. (1999) Bleaching of bacteriorhodopsin by continuous light. *FEBS Lett.* **450**, 154–157
33. Oesterhelt, D. and Stoeckenius, W. (1974) Isolation of the cell membrane of *Halobacterium halobium* and its fractionation into red and purple membrane. *Methods Enzymol.* **31**, 667–678
34. Rehorek, M. and Heyn, M.P. (1979) Binding of all-*trans*-retinal to the purple membrane. Evidence for cooperativity and determination of the extinction coefficient. *Biochemistry* **18**, 4977–4983